Special Collection

The Role of Peripheral Amide Groups as Hydrogen-Bonding Directors in the Tubular Self-Assembly of Dinucleobase Monomers

Violeta Vázquez-González,[a] María J. Mayoral,[a, b] Fátima Aparicio,[a] Paula Martínez-Arjona,[a] and David González-Rodríguez*[a, c]

Nanotubes are a fascinating kind of self-assembled structure which have a wide interest and potential in supramolecular chemistry. We demonstrated that nanotubes of defined dimensions can be produced from dinucleobase monomers through two decoupled hierarchical cooperative processes: cyclotetramerization and supramolecular polymerization. Here we analyze the role of peripheral amide groups, which can form an array of hydrogen bonds along the tube axis, on this self-assembly process. A combination of ^{1}H NMR and CD spectroscopy techniques allowed us to analyze quantitatively the thermodynamics of each of these two processes separately. We found out that the presence of these amide directors is essential to guide the polymerization event and that their nature and number have a strong influence, not only on the stabilization of the stacks of macrocycles, but also on the supramolecular polymerization mechanism.

Chemists are increasingly motivated to design novel nanotubular systems, due to their wide diversity of functions,[1] their nanometer-scale dimensions, and their high aspect ratio. In fact, tube-forming proteins, such as tubulin or aquaporin, or viruses like the tobacco mosaic virus, are seen as a truly amazing category of self-assembled systems with biological functions. Possible applications of such materials with nanospaces of confined dimensions[2] involve molecular sieve technologies,[2b] chemo- and size-selective encapsulation and storage, catalysis and sensing,[2a] or biomedical applications, such as drug transport and biological ion channel mimics.[2c–e]

Probably the most important aspects in the design of nanotubes or nanotube networks are the modulation of their dimensions (i.e., adjusting the inner pore, tuning nanotube diameter), as well as ruling internal and external functionality. In this context, self-assembled nanotubes and nanochannels built from organic molecules arise as promising materials that offer some distinct advantages with respect to carbon, inorganic or polymeric[3] materials. These include low-cost preparation under equilibrium conditions, synthetic versatility, biocompatibility, as well as precise tailoring of structure and function.[3–4] Inspired by natural systems, the idea is to program molecules with the required chemical information so that they spontaneously assemble into well-defined tubular structures via a combination of non-covalent interactions and cooperative effects.[5]

In this context, we recently reported on the self-assembly of dinucleobase rod-like monomers like **GC1** (Figure 1a), comprising complementary G and C bases at the edges, into tubular structures[6] in alkane solvents.[6a] Remarkably, this assembly process occurred through two decoupled cooperative steps of

[a] Dr. V. Vázquez-González, Dr. M. J. Mayoral, Dr. F. Aparicio, P. Martínez-Arjona, Prof. D. González-Rodríguez
Nanostructured Molecular Systems and Materials Group
Organic Chemistry Department, Science Faculty
Universidad Autónoma de Madrid
28049 Madrid (Spain)
E-mail: david.gonzalez.rodriguez@uam.es
[b] Dr. M. J. Mayoral
Inorganic Chemistry Department
Chemistry Faculty
Universidad Complutense de Madrid
28040 Madrid (Spain)
[c] Prof. D. González-Rodríguez
Institute for Advanced Research in Chemical Sciences (IAdChem)
Universidad Autónoma de Madrid
28049 Madrid (Spain)

Supporting information for this article is available on the WWW under https://doi.org/10.1002/cplu.202100255

Special Collection This article is part of a Special Collection celebrating the 10th Anniversary of ChemPlusChem.
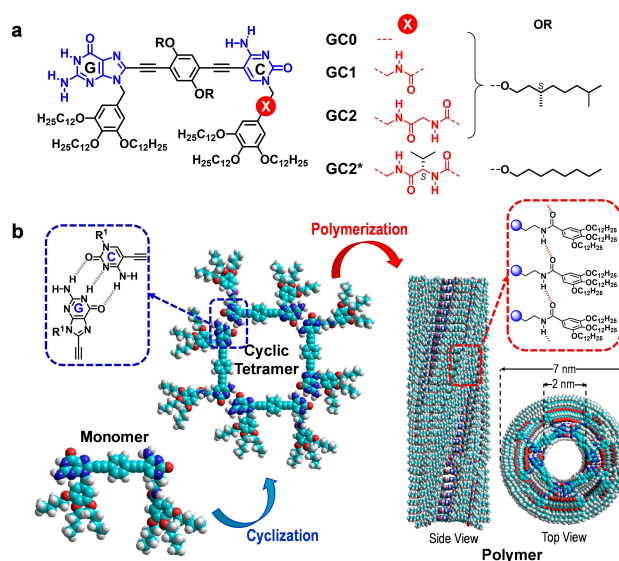
Figure 1. (a) Structure of S-chiral **GC0**–**GC2** molecules (see also Figure 2). (b) Scheme of the two-step self-assembly of dinucleobase monomers.

ChemPlusChem

Communications
doi.org/10.1002/cplu.202100255

Chemistry
Europe

European Chemical
Societies Publishing

different hierarchy (Figure 1b): 1) a cyclotetramerization process[7] controlled by Watson-Crick G:C pairing and enjoying a high chelate cooperativity,[8] and 2) a supramolecular polymerization in which the macrocycles orderly stack to generate the final nanotubes through a nucleation-elongation mechanism.

The peripheral amide group placed at the C base in **GC1** was suspected to play a key role along the polymerization phase, stabilizing **GC1** tubular stacks by formation, just like in peptide β-sheets, of an array of H-bonds parallel to the tube's main axis, so we called them "parallel directors". Here, we analyze the influence of these groups on this self-assembly process. We prepared three other related monomers (Figure 1a) endowed with 0 (**GC0**) or 2 (**GC2** and **GC2***) peripheral amides and studied their self-organization, focusing on both the cyclotetramerization and the polymerization processes. We reveal that these parallel directors are indeed crucial to trigger polymerization, and that they greatly contribute to the stabilization of the tubular assemblies.

Synthesis. Monomers **GC0**–**GC2** are endowed with a *p*-phenylene central block having lateral alkyl chains with *S*-chiral centers, and thus only differ in the number of peripheral amide groups placed at the C unit. Monomer **GC2*** is analogous to **GC2**, but we moved the chiral center to the lateral chain at the C base by installing a valine derivative. However, despite showing a similar association behavior as **GC2**, evolving from a cyclic tetramer structure to longitudinal aggregates of the expected diameter (see below), the assemblies of **GC2*** turned

out to be inactive in CD, an essential technique used in these studies, so we discarded this compound for subsequent experimental comparisons. The synthesis and molecular characterization of the cytosine precursors, as well as the novel dinucleobase monomers **GC0**, **GC2** and **GC2*** (Scheme 1), is detailed in the Experimental Section, as well as in the Supporting Information.

The synthesis of **GC1** and the rest of nucleobase and central block precursors can be found in our previous work.[6a] Cytosine **C0**[9] was prepared from 5-iodocytosine by an alkylation reaction with the benzylic wedge **W0**,[10] followed by installation of the terminal acetylene *via* Sonogashira coupling with trimethylsilylacetylene (TMSA) and subsequent deprotection of the trimethylsilyl (TMS) group in the presence of fluoride ions. On the other hand, precursors **C2** and **C2*** were prepared from the amine-protected cytosine **C2.1**[9] by Boc-deprotection, and subsequent condensation reaction with acids **W2**[11] or **W2***, respectively, whose preparation is further detailed at the S.I. Then, monomers **GC0**, **GC2** and **GC2*** were synthesized by two consecutive Sonogashira cross-couplings between diiododerivatives **B**[12] or **B1**[13] and, firstly, the 5-ethynylcytosines **C0**, **C2** and **C2***, to yield the corresponding monocoupled products, and, subsequently, the 8-ethynylguanine **G**,[9,14] to arrive to the final monomers.

The cyclotetramerization process. As stated in the Introduction, when these GC dinucleobase molecules are gradually exposed to experimental conditions that favor their association
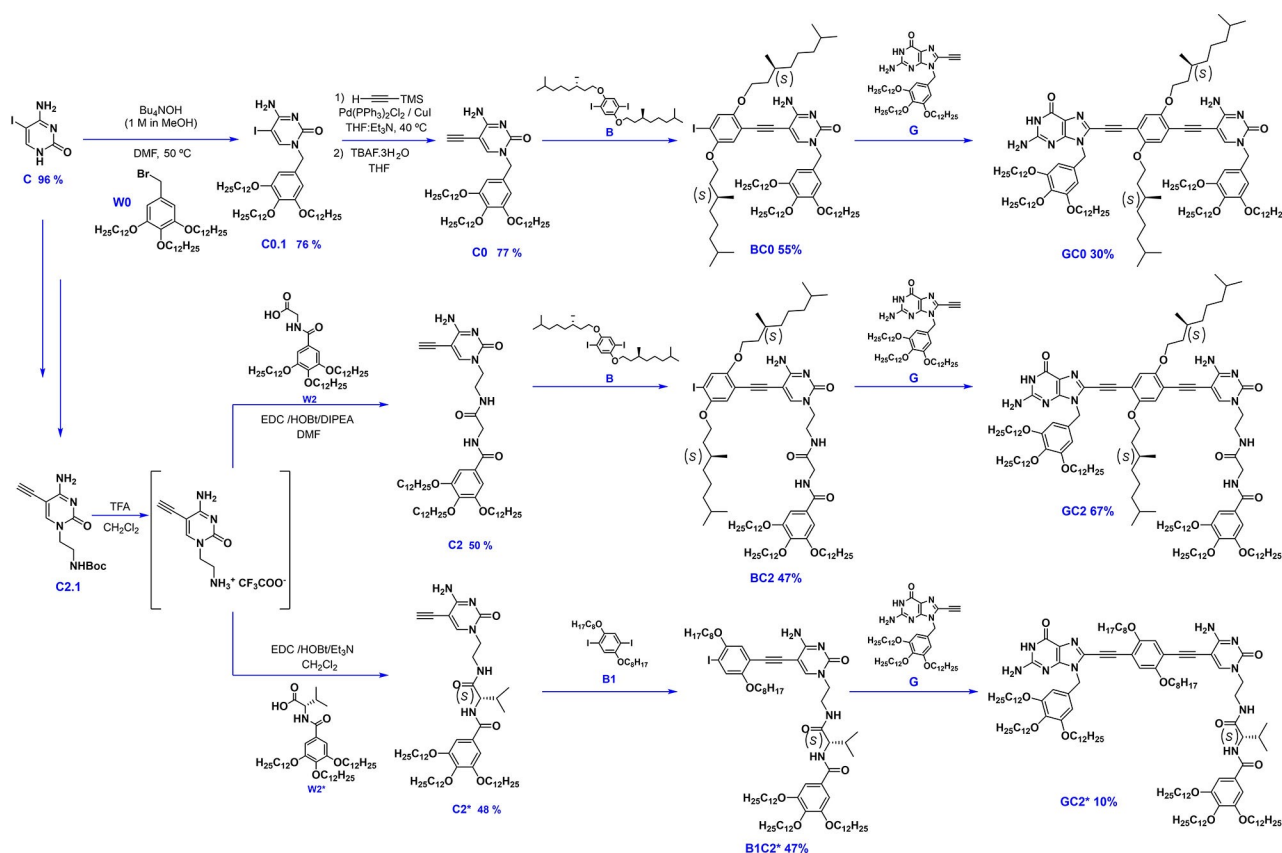
Scheme 1. Synthesis of the new cytosine derivatives **C0**, **C2** and **C2*** and final monomers **GC0**, **GC2** and **GC2***.

ChemPlusChem

Communications
doi.org/10.1002/cplu.202100255

**Chemistry
Europe**
European Chemical
Societies Publishing

by H-bonding, a cyclotetramerization process, guided by G:C Watson-Crick pairing interactions, is triggered first without actually observing oligo/polymerization through monomer stacking. Such monomer (GC) - cyclotetramer (c(GC)$_4$) equilibrium was studied by a number of spectroscopic techniques. From our experience[6a] and preliminary studies (Figure S1), a solvent of intermediate polarity like THF is the best candidate to study the cyclotetramerization process, which can be principally done with ^{1}H NMR, CD and emission spectroscopies. Since all macrocycles are formed from similar complementary G and C nucleobases, we expected that the association process of all monomers during this first equilibrium would be comparable, at least qualitatively.

Temperature- and concentration-dependent ^{1}H-NMR experiments in THF-d$_8$ (Figures 2a–c and S2A, C) were first carried out in order to calculate the molar fraction of c(GC)$_4$ species in diverse conditions and to evaluate the thermodynamic stability of each cyclic tetramer. In all cases, the G-amide and C-amine proton signals were detected at around 13.5 and 10.0 ppm (see Figures S2A, C), which is typical for H-bonded G:C pairs. High temperatures and low concentrations favor dissociation into GC monomers while low temperatures and high concentrations obviously promote c(GC)$_4$ formation. It is interesting to remark that, for all monomers, only these two species were detected in slow exchange in the NMR timescale, and no sign of small open oligomeric species was noticed, highlighting the strong *all-or-nothing* cooperativity of the cyclotetramerization process. CD experiments in the same conditions (Figures 2d–f and S2B, D) were in agreement with the NMR results. As described in previous work, CD spectroscopy turns out to be also very informative to assess the formation of cyclic species along our whole studies with dinucleoside monomers.[6a,8a,e] This kind of molecules can switch between different conformations by rotation around the σ-bonds in their rigid π-framework, that dispose the nucleobase Watson-Crick edges either at the same side or at opposite sides of the molecule. Upon cyclotetramerization, this degrees of freedom are lost and the Watson-Crick faces at the edge nucleobases are blocked and forced to point to the same side. Such conformational "locking" might enhance the interaction between the chiral groups and the π-conjugated backbone, so that the system becomes CD active. Hence, the CD trends recorded upon cyclization can be used to detect and analyze quantitatively the cyclotetramerization process in a complementary way and in a lower concentration range, because non-cyclic or non-associated species are CD-inactive.[8] The fixation of the planar *syn* conformation upon cyclotetramerization also explains the marked red-shifts observed in the absorption and emission spectra (see Figure S1). So, in the same experimental conditions, the cyclotetramerization trends monitored by ^{1}H NMR and CD as a function of temperature or concentration closely overlap, as shown in Figures 2g and S2F.
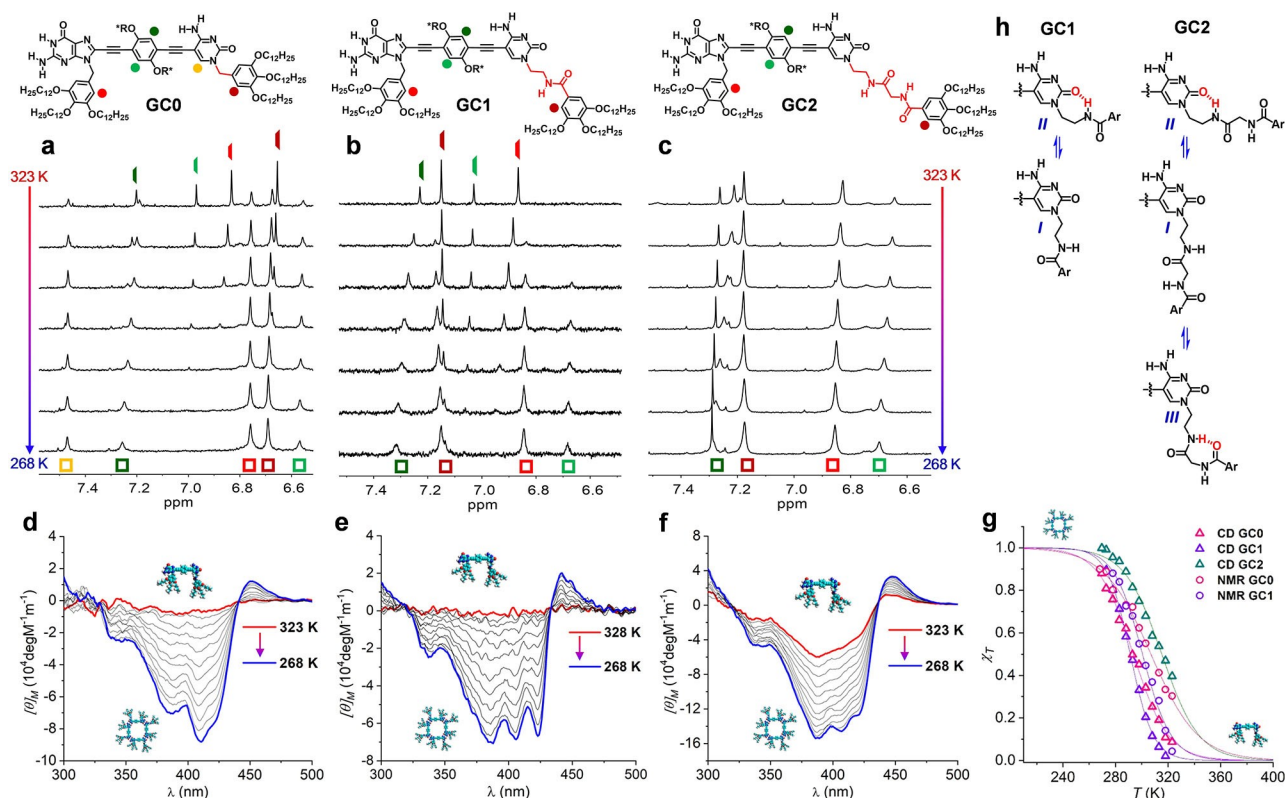

Figure 2. (a–c) Chemical structure and aromatic region of the ^{1}H NMR spectra in THF-d$_8$ and (d–f) CD spectra in THF of compounds (**a**, **d**) **GC0**, (**b**, **e**) **GC1**, and (**c**, **f**) **GC2** as a function of the temperature. In all cases $C = 1.0 \cdot 10^{-4}$ M. c(GC)$_4$ and GC proton signals are marked with colored squares or rods, respectively. (**g**) Representation of the molar fraction of molecules associated as c(GC)$_4$ cycles (χ_T) calculated by ^{1}H NMR (circles) or CD (triangles) as a function of the temperature. (**h**) Possible conformations adopted by the amide substituents at the C base. In some of them an intramolecular H-bond may be formed leading to 7- (*II*) or 6-membered (*III*) rings.

ChemPlusChem

Communications
doi.org/10.1002/cplu.202100255

**Chemistry
Europe**
European Chemical
Societies Publishing

However, each macrocycle displayed a markedly different stability: $c(GC2)_4 > c(GC0)_4 > c(GC1)_4$. For instance, at 298 K and at an identical 10^{-4} M concentration in THF, the molar fraction of molecules associated as cyclic tetramers (χ_T) was > 0.9 for **GC2**, 0.75 for **GC0** and 0.55 for **GC1**. These χ_T values as a function of concentration and temperature allowed us to calculate the cyclotetramerization constant (K_T) and, through van't Hoff plots (Figure S2G), the corresponding enthalpy (ΔH) and entropy (ΔS) changes associated to the cyclotetramerization equilibria, which are compared in Table 1a. The only exception was **GC2**, for which, due to the strong association in these conditions, only a lower K_T limit could be determined.

In order to compare the cooperativity of each cyclotetramerization process, the corresponding reference association constants for each G:C nucleobase pair ($K_{G:C}$)[15] were measured in separate titration experiments (see Figure 3 and S3 A), and the effective molarity (*EM*) was calculated using the relationship $K_T = EM \cdot K_{G:C}^4$. Thus the noted differences in cycle stability may either come from a different *EM* for each cycle, from the subtle differences in G:C association constants that the lateral substituents at the C nucleobase may cause, or from a contribution of both parameters. From the data shown in

Table 1a, it is clear that, even if there are not important differences in $K_{G:C}$, the fact that each cycle is bound by 4 G:C interactions, and thereof $K_{G:C}$ is raised to the 4th power in the equation, can already explain the notable differences in cycle stability. The calculated *EM* values are, on the other hand and as expected, very similar for each cycle and in the order of 10^2 M, thus in the same range as those calculated for related cycles made from G–C dinucleosides.[8a]

The polymerization process. We next investigated the supramolecular polymerization to yield self-assembled nanotubes. This is a second stage in the overall self-assembly landscape of these GC dinucleobase monomers that is only triggered when the molecules are exposed to experimental conditions that really increase their degree of aggregation, like in highly apolar solvents. In such conditions, as was demonstrated for **GC1** in our previous work,[6a] and as will be proven below for the rest of GC molecules studied in this work, the cyclic tetramers are already formed quantitatively, meaning that both processes (i.e., cyclotetramerization and supramolecular polymerization) are totally decoupled. The number of peripheral amides is expected to play an important role in this polymerization process, since they should be involved in enhancing

Table 1. Thermodynamic parameters calculated for **GC0–GC2** upon (**a**) cyclotetramerization and (**b**) polymerization as a function of temperature.

a		$K_{G:C}$[a] [M^{-1}]	K_T[b] [M^{-3}]	*EM*[c] [M]	ΔH_T[d] [kJ·mol^{-1}]	ΔS_T[e] [J·mol^{-1}·K^{-1}]
GC0		$0.55 \cdot 10^3$	$4.3 \cdot 10^{13}$	$4.7 \cdot 10^2$	-143.4	-215.1
GC1		$0.41 \cdot 10^3$	$3.4 \cdot 10^{12}$	$1.2 \cdot 10^2$	-173.4	-331.2
GC2		$0.77 \cdot 10^3$	$> \cdot 10^{14}$	$> 2.8 \cdot 10^2$	[f]	[f]

b	T_e[g] [K]	K_n[h] [M^{-1}]	K_e[i] [M^{-1}]	σ[j]	ΔH^{0}[k] [kJ·mol^{-1}]	ΔS^{0}[l] [J·mol^{-1}·K^{-1}]
GC1	298	$4.0 \cdot 10^1$	$1.3 \cdot 10^5$	$3.0 \cdot 10^{-4}$	-116 ± 3	-290 ± 10
	T_m[m] [K]	K [M^{-1}]			ΔH^{0}[k,n] [kJ·mol^{-1}]	ΔS^{0}[k,n] [J·mol^{-1}·K^{-1}]
GC2	279	$4.0 \cdot 10^4$		1	-83 ± 2	-192 ± 6

[a] Reference G:C association constant calculated in separate experiments (see Figures 3 and S3A). [b] Cyclotetramerization constant. [c] Effective molarity calculated as: $EM = K_T / K_{G:C}^4$. [d] Cyclotetramerization enthalpy and [e] entropy. [f] Could not be determined. [g] Elongation temperature at $3.0 \cdot 10^{-5}$ M. [h] Nucleation and [i] elongation constants, [j] cooperativity factor, and elongation [k] enthalpy and [l] entropy of the polymerization process. [m] Melting temperature calculated from the isodesmic model. [n] Calculated using the van't Hoff equation.
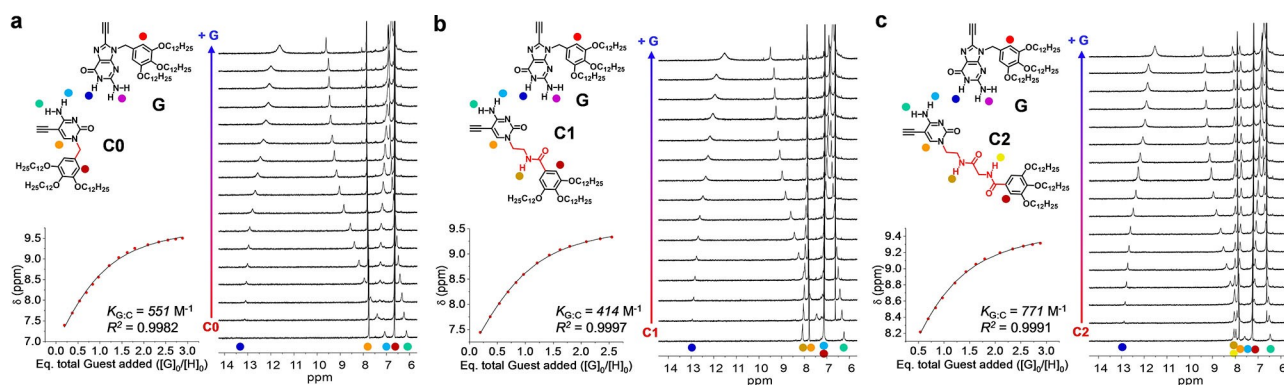

Figure 3. ^{1}H NMR titration experiments of **G** (guest) over (**a**) **C0**, (**b**) **C1**, or (**c**) **C2** (host) at a constant host concentration of 5 mM in THF-d$_8$. The corresponding fittings to a 1:1 model are shown at the left.

ChemPlusChem

Communications
doi.org/10.1002/cplu.202100255

Chemistry
Europe

European Chemical
Societies Publishing

stacking interactions between the macrocycles, thus contributing to the stabilization of the resulting nanotubes. As also shown in our previous work,[6a] both the cyclotetramerization and polymerization processes can be monitored by CD, absorption or emission spectroscopy. When analyzing and comparing the trends taken from each technique, they perfectly overlap at any concentration and provide virtually the same thermodynamic data. However, CD is the technique that provides a higher difference between cyclotetramer and polymer spectroscopic features, both visually and for quantitative analyses.

We first monitored the spectroscopic changes occurring upon increasing the volume fraction of heptane (V_h) in mixtures with THF, from $V_h = 0$ to $V_h = 0.99$, at different concentrations (Figures 4a–c and S4A–C). As shown in Figure 4d, two processes were observed for **GC1** and **GC2** upon increasing V_h: the monomer-macrocycle equilibrium was monitored from $V_h = 0$ to ca. 0.4-0.5. At that point a CD spectrum that is virtually identical for all molecules is obtained, with a strong negative signal and a weak, positive Cotton effect with zero-crossing at ca. 439 nm.

Then, a plateau is reached up to $V_h = 0.7$–0.8 in which this CD spectrum remains invariable, meaning that the $c(GC)_4$ tetramers are the only species in solution. The supramolecular polymerization of the tetramers was then activated at higher heptane contents. This is experimentally observed by a drastic change in the CD spectra, and the stacked tubular polymers now show a strong bisignated signal with zero-crossing at ca. 428 nm. Interestingly, the polymerization of $c(GC2)_4$, with two peripheral amides per monomer, took place at a significantly lower bad solvent content ($V_h = 0.7$) than the polymerization of $c(GC1)_4$ ($V_h = 0.85$), which is endowed with a single amide per monomer. On the contrary, for **GC0**, devoid of these peripheral H-bonding groups, only the cyclotetramerization process was recorded, and this compound remained associated as $c(GC0)_4$ cyclic tetramers even in pure heptane. These findings indicated that the presence and number of peripheral amides plays indeed a key role in the formation of the polymeric nanotubes. At this point, it is interesting to note that **GC2*** shows a polymerization process somewhat less favourable than **GC2**, most likely as a result of a higher steric hindrance caused by the isopropyl
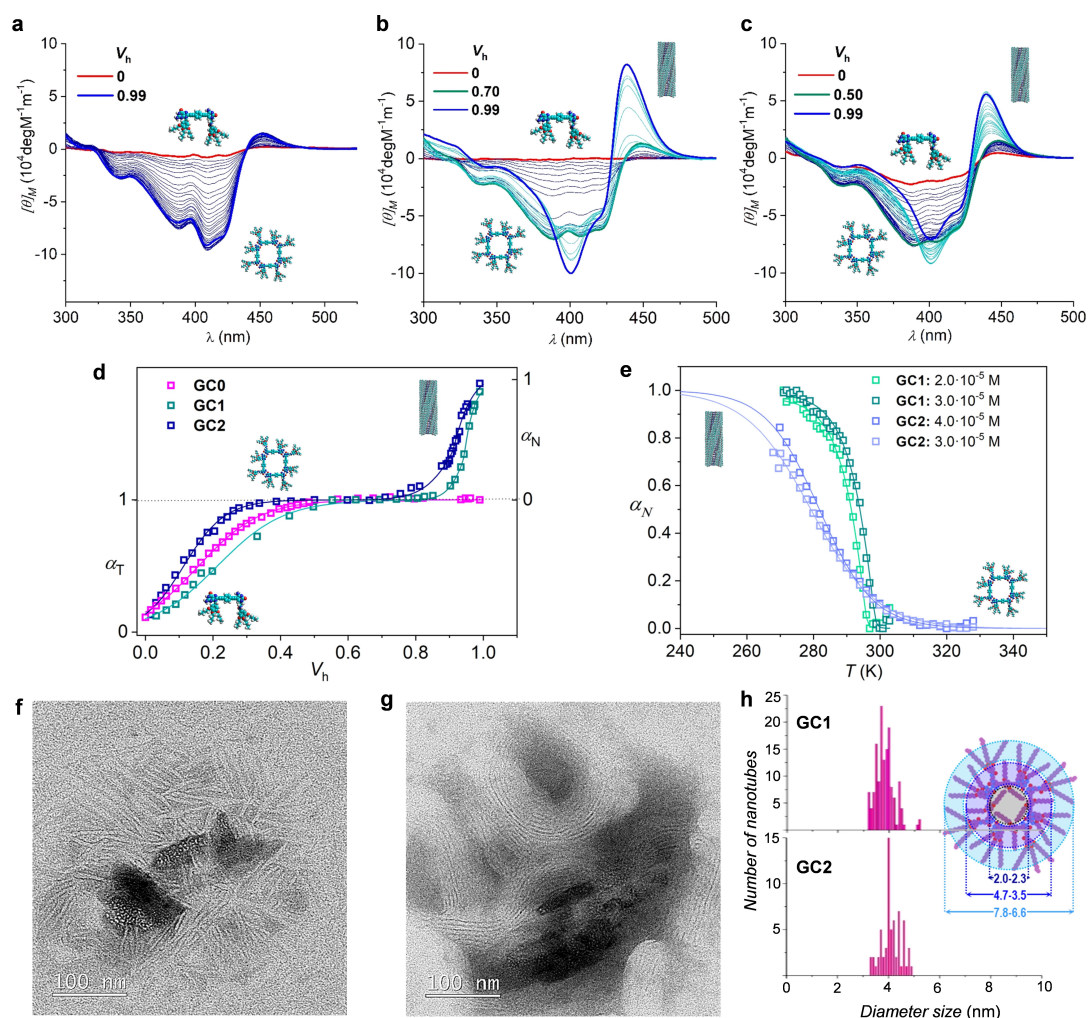

Figure 4. (a–c) Changes observed in the CD spectra as a function of the volume fraction of heptane (V_h) in mixtures with THF for (a) **GC0**, (b) **GC1**, and (c) **GC2** ($C = 3.0 \cdot 10^{-5}$ M; $T = 298$ K). Normalized CD changes at 429 nm as a function of (d) V_h for **GC0-GC2** or (e) the temperature for **GC1** and **GC2**. (α_T = fraction of cyclotetramers, α_N = fraction of aggregated nanotubes). (f,g) TEM images of the assemblies formed by **GC2** drop-casted from diluted solutions of high V_a. (h) Nanotube diameter distribution measured by TEM and dimensions calculated from models.

ChemPlusChem

Communications
doi.org/10.1002/cplu.202100255

Chemistry
Europe
European Chemical
Societies Publishing

group around the amide director. Although we could not record **GC2***'s CD changes, we could compare the supramolecular behaviour of this molecule with the one shown by **GC2** in denaturalization experiments by increasing the volume fraction of THF in heptane at a constant temperature and concentration, monitored by absorption spectroscopy (Figure S4F).

In order to have a deeper insight into the polymerization of $c(GC1)_4$ and $c(GC2)_4$, we conducted temperature-dependent measurements monitored by CD and absorption at different concentrations and at a fixed solvent composition, which was chosen in each case so as to cover as much of the polymerization process as possible within the experimental temperature range ($V_h = 0.97$ for **GC1** and $V_h = 0.81$ for **GC2**; Figures 4e and S4E). As expected, the polymerization process is dependent on concentration and the elongation temperature decreases as the sample is concentrated and with the number of peripheral amides, indicating again a strongest association for **GC2** than for **GC1**. But surprisingly, the shape and the underlying analysis of the cooling curves revealed drastically different polymerization mechanisms. **GC1** exhibited a cooperative polymerization that was analyzed by a nucleation–elongation model,[16] which allowed us to calculate the most important thermodynamic parameters (see Tables 1b and S2),[6a] and revealed a small cooperativity factor (σ). On the contrary, **GC2** (and **GC2***, see Figure S4F) displayed sigmoidal features that were analyzed by the isodesmic model, with $\sigma = 1$.[17]

Although we do not have a clear explanation, we believe this difference is more likely due to the nature of the peripheral C substituents than to the fact that each cooling curve was measured at a different V_h. As shown in Figure 2h, the pendant groups at the C base can adopt different conformations. In some of them the amide groups are bound to solvent molecules and in some others intramolecular H-bonds can be established.[18] We discard the formation of intermolecular H-bonds between these amides at high THF contents, since their chemical shifts do not change with concentration (Figure S2C). A quite probable conformation for **GC1** and **GC2**, where a 7-membered H-bonded ring is formed intramolecularly, is represented in Figure 2h as conformation *II*. However, upon Watson-Crick pairing, such conformation must become much less populated, because the C-carbonyl group needs to bind the G base as well. Hence, cyclization would "release" such amide group, which would be available for polymerization. However, in **GC2**, a different kind of intermolecular H-bond leading to a 6-membered ring can be expected (conformation *III*), which might "sequester" the amide group and thus influence the polymerization mechanism.

We made a number of experiments to try to get a deeper insight into this issue without much success. On one hand, ^{1}H NMR spectra down to 178 K were acquired with the individual C nucleobases (**C1** and **C2**; see Figure S3B), to try to "freeze" one of these conformations and detect it in slow exchange. However, the compounds precipitated below 218 K and the amide signals (and actually all protons involved in H-bonding interactions) only showed a gradual downfield shift with decreasing temperature (see also Figure S2A). On the other

hand, we recorded different ^{1}H NMR spectra at gradually increasing volume fractions of cyclohexane-d_{12} into THF-d_8, with the aim to see a change in the amide chemical shifts just when polymerization is triggered. However, when $c(GC1)_4$ and $c(GC2)_4$ start to polymerize, their ^{1}H NMR signals become too broad and disappear before any H-bonding rearrangement can be detected (Figure S2E). FT-IR spectroscopy experiments performed in THF or THF:heptane (1:99) solutions or in the solid state (see Section S0 at the Supporting Information) did not help in providing further information either about the nature of the most abundant conformation in each of these situations. We analyzed both the amine/amide N–H region between 3000 and 3600 cm^{-1} and the carbonyl region between 1500 and 1800 cm^{-1}. However, the high number of functional groups present in each monomer makes this analysis extremely difficult. For instance, a monomer like **GC2** has 4 C=O groups, 2 exocyclic NH_2 groups and 3 N–H amide groups. Besides, depending on the conditions, some of these groups may be H-bonded intramolecularly, intermolecularly, or some may be bound to solvent molecules, while some other may not be H-bonded. We tried to simplify the system by comparing first the nucleobase fragments **C0**, **C1**, **C2** and **G**, but even there, no final conclusion could be obtained.

Finally, we drop-casted **GC1**, **GC2** and **GC2*** samples from diluted solutions with $V_h > 0.8$, and analyzed them by TEM. As Figures 4f-h and S5 demonstrate, longitudinal objects with a measured diameter of 3.9 ± 0.7 nm (**GC1**) or 4.0 ± 0.8 nm (**GC2**), which coincides with the hard aromatic section of the cyclic tetramers, were imaged. We also noted that it is quite frequent to observe aligned nanotube bundles, especially as the time in solution before deposition becomes longer, which would be the result of van der Waals interactions between the peripheral alkyl chains of individual nanotubes. As a matter of fact, in some cases, especially if the sample concentration is high, we observed nanotube precipitation with time at the highest V_h values. It is important to note that SAXS and DLS measurements, as shown in our previous work for **GC1**,[6a] were in agreement with the formation of large cylindrical aggregates with a cylinder diameter of 4 ± 1 nm and a core diameter of about 1 nm.

In this work we focused on the analysis of the influence of the nature of the directors placed at the C base on the thermodynamics of the supramolecular processes to build self-assembled nanotubes. We focused separately on the cyclo-tetramerization and the supramolecular polymerization events. We noted that these substituents lead to slight deviations in the association constants between G and C nucleobases that can however have a strong impact on macrocycle stability. More importantly, the presence of these amide groups is essential to trigger and guide the stacking of the $c(GC)_4$ "supramonomers", while their number greatly influences tube stability. Unexpectedly, the supramolecular polymerization mechanism is also modulated by these external groups, probably through a competition between intra- and intermolecular H-bonding equilibria.

ChemPlusChem

Communications
doi.org/10.1002/cplu.202100255

**Chemistry
Europe**
European Chemical
Societies Publishing

Experimental Section

General Methods: Mass Spectrometry (MS) and High Resolution-Mass Spectrometry (HRMS) MALDI-TOF spectra were obtained from a BRUKER ULTRAFLEX III instrument equipped with a nitrogen laser operating at 337 nm. NMR spectra were recorded with a *BRUKER AVANCE-II* 300 MHz or a *BRUKER DRX* 500 MHz instrument. The temperature was actively controlled at 298 K. Chemical shifts are measured in ppm using the signals of the deuterated solvent as the internal standard [CDCl$_3$ calibrated at 7.26 ppm (^{1}H) and 75.0 ppm (^{13}C), DMSO-d$_6$ calibrated at 2.50 ppm (^{1}H) and 39.5 ppm (^{13}C) and THF-d$_8$ calibrated at 3.58 (^{1}H) and 39.5 ppm (^{13}C)]. Due to solubility problems the ^{13}C-NMR data for some final monomers and their derivatives could not be performed. Column chromatography was carried out on silica gel *Merck-60* (230–400 mesh, 60 Å), and TLC on aluminium sheets precoated with silica gel 60 F254 (Merck). FT-IR spectra were recorded with a *PerkinElmer* spectrometer UATR two. UV-Visible experiments were conducted using a *JASCO V-660* apparatus. Emission spectra were recorded in a *JASCO FP-8600* equipment using excitation and emission bandwidths of 5 nm in both cases, and a 50 ms response. CD spectra were recorded with a *JASCO* J-815 equipment. The slit width was set at 1000 μm and a DIT of 2 s was used. In all these three instruments the temperature was controlled using a *JASCO* Peltier thermostatted cell holder with a range of 263–383 K, adjustable temperature slope, and accuracy of ± 0.1 K. Transmission electron microscopy (TEM) images were obtained with a *JEOL-JEM 1010* instrument operating at 100 kV for the stained samples and a *JEM 1400K PLUS* instrument operating at 100 kV for non-stained samples.

Standard procedures

Standard Procedure A for the nucleobase alkylation reaction. To a suspension of the nucleobase starting material (1 eq) and a base (1.2 q) (indicated in each case) in dry DMF (volume indicated in each case) the corresponding iodoalkane or benzyl bromide/chloride (1.2 eq) (indicated in each case) was added dropwise. The mixture was stirred under argon at 40°C for a period of time (indicated in each case) until completion, which was monitored by TLC. Work-up and purification methods are also indicated in each case.

Standard Procedure B for the Sonogashira coupling with TMSA and subsequent alkyne-TMS group deprotection. A dry THF/Et$_3$N (4:1) solvent mixture was subjected to deoxygenation by three freeze-pump-thaw cycles with argon. Then, this solvent was added to the system containing the corresponding halogenated base (1 eq), CuI (0.01 eq) and Pd(PPh$_3$)$_2$Cl$_2$ (0.02 eq). The mixture was stirred at room temperature for a few minutes. Then, trimethylsilylacetylene (TMSA; 2 eq) was added dropwise. The reaction was stirred under argon at a given temperature for a period of time (indicated in each case) until completion, which was monitored by TLC. Then, the mixture was filtrated over celite and the solvent evaporated under vacuum. The resulting crude was placed in a round-bottom flask equipped with a magnetic stirrer, followed by addition of THF and the mixture was stirred at room temperature until the solid was dissolved. Then, hydrated tetrabutylammonium fluoride (TBAF·3H$_2$O; 1 eq) was slowly added at 0°C. The mixture was allowed to reach room temperature and it was stirred until its completion, which was monitored by TLC (approximately 1 hour in all cases). The solvent was evaporated at reduced pressure and the product was purified by column chromatography (eluent indicated in each case). The resulting solid was finally washed with cold acetonitrile.

Standard Procedure C for the Sonogashira coupling with ethynyl-nucleobases. A dry THF or THF/NEt$_3$ solvent mixture (indicated in

each case) was subjected to deoxygenation by three freeze-pump-thaw cycles with argon. Then, this solvent was added over the system containing the corresponding ethynyl-substituted base (quantity indicated in each case), iodoarene derivative (quantity indicated in each case), CuI (0.01 eq) and PdCl$_2$(PPh$_3$)$_2$ or Pd(Ph$_3$)$_4$ (0.02 eq). The mixture was stirred under argon at 40°C (unless indicated otherwise) until completion, which was monitored by TLC. The purification methods are explained in each case.

Starting materials. Chemicals were purchased from commercial suppliers and used without further purification. Solid hygroscopic reagents were dried in a vacuum oven before use. Reaction solvents were thoroughly dried before use using standard methods. The synthesis and characterization of compounds **W**,[19] **W0**,[10] **W2**,[11] **C2.1**,[9] **C**,[9] **B**,[12] **B1**,[13] **G**[9] and **GC1**[6a] have already been described in the literature.

Synthetic procedures and characterization data of the nucleobase substituents (W2*, Scheme S1)

W2.1*: To a solution of the acid **W**[19] (3.0 g, 4.5 mmol) in dry CH$_2$Cl$_2$ (50 mL) at 0°C, EDC (1.7 g, 9.0 mmol) and HOBt (1.2 g, 9.0 mmol) were added, and then the solution was stirred for ten minutes. In another flask, a solution of the aminoacid (1.1 g, 6.7 mmol) and Et$_3$N (1.2 mL, 9.0 mmol) in CH$_2$Cl$_2$ (40 mL) was stirred for 15 minutes, and then added to the solution of the acid. Once the addition was completed the ice bath was removed, the resulting solution was stirred at room temperature overnight. Once the reaction was completed, the solution was diluted with CH$_2$Cl$_2$ and then washed with HCl (0.1 N), NaHCO$_3$ (sat) and NaCl (sat). The phases were separated and the organic layer was dried with Na$_2$SO$_4$. Finally, the solvent was evaporated under reduced pressure, and the resulting product was purified by column chromatography using AcOEt/Cyclohexane (1:6) as eluent. The desired product was obtained as a white solid (3.2 g, 90%). ^{1}H-NMR (300 MHz, CDCl$_3$) $\delta = 6.99$ (s, 2H, H^1), 6.52 (d, $J = 8.7$ Hz, 1H, NH), 4.75 (dd, $J = 8.6$, 5.0 Hz, 1H, CH^2), 4.00 (q, $J = 6.8$ Hz, 6H, OCH_2), 3.77 (s, 3H, OCH_3), 2.26 (td, $J = 6.9$, 5.0 Hz, 1H, H^3), 1.77 (ddd, $J = 21.3$, 8.5, 6.3 Hz, 6H, OCH$_2$CH_2), 1.60–1.27 (m, 54H, OCH$_2$CH$_2$(CH_2)$_9$CH$_3$), 0.99 (t, $J = 6.8$ Hz, 6H, CH_3^4), 0.93–0.81 (m, 9H, O(CH$_2$)$_{11}$CH_3) ppm. ^{13}C-NMR (75 MHz, CDCl$_3$) $\delta = 172.7$, 167.0, 153.0, 141.5, 128.9, 105.9, 73.4, 69.3, 57.5, 52.0, 31.9, 31.5, 30.2, 29.7, 29.61, 29.57, 29.55, 29.50, 29.31, 29.28, 26.0, 22.6, 18.9, 18.0, 14.0 ppm. MS (ESI$^+$): Calculated for C$_{49}$H$_{89}$NO$_6$: 788.23; found: 789.69 [M+H]$^+$. [α]D$_{20}$ = +11.78 (c = 1, CHCl$_3$).

W2*: To a suspension of the ester **W2.1*** (788.0 mg, 1.0 mmol) in MeCN (40 mL) at room temperature, NaOH 2N (3.2 mL, 6.5 mmol) was added, and the solution was then heated at 40°C overnight. Once the reaction was completed, the solvent was removed under reduced pressure. The crude product was dissolved in CH$_2$Cl$_2$ and the solution was acidified until pH 3 was reached. The solution was then washed with NaCl and dried with Na$_2$SO$_4$. The evaporation of the solvent led to the final product (735.3 mg, 95%). ^{1}H-NMR (300 MHz, CDCl$_3$): $\delta = 9.57$ (s broad, 1H, OH), 6.99 (s, 2H, H^1), 6.62 (dd, $J = 8.6$, 2.4 Hz, 1H, NH), 4.75 (dd, $J = 8.4$, 4.8 Hz, 1H, H^2), 3.99 (td, $J = 6.5$, 4.9 Hz, 6H, OCH_2), 2.42–2.26 (m, 1H, H^3), 1.96–1.67 (m, 6H, OCH$_2$CH_2), 1.46 (dd, $J = 10.2$, 5.3 Hz, 6H, OCH$_2$CH$_2$CH_2), 1.40–1.21 (m, 48H, OCH$_2$CH$_2$CH$_2$ (CH_2)$_8$CH$_3$), 1.03 (t, $J = 6.9$ Hz, 6H, CH_3^4), 0.97–0.79 (m, 9H, O(CH$_2$)$_{11}$CH_3) ppm. ^{13}C-NMR (75 MHz, CDCl$_3$) $\delta = 175.4$, 167.6, 152.9, 141.5, 128.3, 105.8, 73.3, 69.2, 57.4, 31.6, 31.0, 30.0, 29.42, 29.40, 29.38, 29.36, 29.34, 29.3, 29.12, 29.08, 29.06, 25.81, 25.78, 22.4, 18.8, 17.7, 13.8 ppm. MS (ESI$^+$): Calculated for C$_{48}$H$_{89}$NO$_6$: 775.67 [M+H]$^+$; found: 775.67 [M+H]$^+$. [α]D$_{20}$ = +14.89 (c = 1, CHCl$_3$).

ChemPlusChem

Communications
doi.org/10.1002/cplu.202100255

Chemistry Europe
European Chemical
Societies Publishing

Synthetic procedures and characterization data for the new cytosine derivatives (C0, C2 and C2*, Schemes 1 and S2)

C0.1. Following *Standard Procedure A*, to a solution of **C**[9] (1.0 g, 4.2 mmol) in dry DMF (100 mL), a 1.0 M solution of Bu_4NOH in MeOH was added (4.2 mL, 4.2 mmol) and the mixture was stirred for 30 minutes at 50 °C. Then, 1-(bromomethyl)-3,4,5-tris(dodecyloxy)benzene (**W0**)[10] (3.4 g, 4.6 mmol) was dissolved in dry DMF (50 mL) and added *via cannula* to the solution. This solution was stirred for 12 h. After completion, the solvent was evaporated under reduced pressure. The residue was purified by column chromatography eluted with $CHCl_3$:MeOH (20:1) to afford **C0.1** as a white solid (2.8 g, 76%). ^{1}H-NMR (300 MHz, $CDCl_3$): $\delta = 9.10$ (s broad, 1H, $C^4NH\text{-}H$), 7.48 (s, 1H, H^6), 6.46 (s, 2H, s, H^2), 5.65 (s, 1H, $C^4NH\text{-}H$), 4.82 (s, 2H, N^1CH_2), 3.92 (t, $J = 6.3$ Hz, 6H, OCH_2), 1.75 (m, 6H, OCH_2CH_2), 1.24 (m, 54H, $OCH_2CH_2(CH_2)_9CH_3$), 0.86 (m, 9H, O-$(CH_2)_{11}CH_3$) ppm. ^{13}C-NMR (75 MHz, $CDCl_3$) $\delta = 165.0$, 155.1, 153.6, 148.3, 138.4, 130.6, 107.1, 90.2, 84.0, 77.3, 75.0, 73.4, 69.3, 52.7, 32.0, 30.4, 29.8, 29.7, 29.5, 26.17, 22.74, 14.2 ppm. HRMS (ESI[+]): Calculated for $C_{47}H_{83}IN_3O_4$: 880.5422 [M+H][+]. Found: 880.5454 [M+H][+]. m. p. 115.4–117.7 °C.

C0. Following *Standard Procedure B*, to a solution of **C0.1** (500.0 mg, 0.6 mmol), $Pd(Ph_3)_2Cl_2$ (7.7 mg, 0.01 mmol), and CuI (1.1 mg, 0.01 mmol) in THF/Et_3N (5 mL), TMSA (1.4 mL, 2.3 mmol) was added and the mixture stirred at 40 °C overnight. Once the reaction was completed, the solvent was evaporated, the resulting crude was suspended in THF (10 mL) and TBAF·$3H_2O$ (625.0 mg, 0.6 mmol) was added. After completion the solvent was evaporated and the resulting residue was purified by column chromatography eluted with $CHCl_3$:MeOH (50:1), affording **C0** as a pale solid (340.0 mg, 77%). ^{1}H-NMR (300 MHz, $CDCl_3$): $\delta = 7.47$ (s, 1H, H^{6C}), 6.87 (s broad, 1H, $C^4NH\text{-}H$), 6.49 (s, 2H, H^2), 5.67 (s broad, 1H, $C^4NH\text{-}H$), 4.87 (s, 2H, N^1CH_2), 3.93 (td, $J = 6.5$, 2.2 Hz, 6H, OCH_2), 3.32 (s, 1H, C≡CH), 1.89–1.52 (m, 6H, OCH_2CH_2), 1.28 (m, 54H, $OCH_2CH_2(CH_2)_9CH_3$), 1.03–0.67 (m, 9H, $O(CH_2)_{11}CH_3$) ppm. ^{13}C-NMR (75 MHz, $CDCl_3$): $\delta = 165.0$, 155.1, 153.6, 148.3, 138.4, 130.6, 107.1, 90.2, 84.0, 77.3, 75.0, 73.4, 69.3, 52.7, 32.0, 30.4, 29.8, 29.7, 29.5, 26.2, 22.7, 14.2 ppm. HRMS (ESI[+]): Calculated for $C_{49}H_{84}N_3O_4$: 778.6456 [M+H][+]. Found: 778.6464 [M+H][+]. m. p. 94.2–95.9 °C.

C2. To a suspension of **C2.1**[9] (270.0 mg, 1.0 mmol) in CH_2Cl_2 (26 mL), TFA (4.0 mL, 51.4 mmol) was added. The resulting solution was stirred at room temperature for 3 h, then TFA was removed by coevaporation with CH_2Cl_2 under reduced pressure. The resulting crude was re-dissolved in dry DMF and stirred at room temperature for 20 minutes, then cooled to 0 °C. Meanwhile, to a solution of the acid **W2**[11] (710.0 mg, 1.0 mmol) in CH_2Cl_2 at 0 °C, EDC (267.2 mg, 1.9 mmol), HOBt (331.2 mg, 2.5 mmol) and DIPEA (0.3 mL, 1.9 mmol) were added. The solution was stirred at room temperature for one hour, the solvent was removed under reduced pressure and the crude re-dissolved with DMF and a few drops of a $CHCl_3$:MeOH (10:1) mixture. This solution was added to the solution at 0 °C of the deprotected amine, and then stirred at room temperature overnight. Once the reaction was completed, the solution was washed with HCl (0.1 M), $NaHCO_3$ (sat) and NaCl (sat). The phases were separated and the organic layer was dried with $MgSO_4$ and the solvent evaporated under reduced pressure. The crude product was purified by column chromatography using a 10:1 $CHCl_3$:MeOH mixture as eluent, affording a white solid (89.1 mg, 50%). ^{1}H-NMR (300 MHz, $CDCl_3$): $\delta = 8.71$ (s broad, 1H, NH^5), 7.81 (s broad,1H, NH^3), 7.46 (s, 1H, H^{6C}), 7.08 (s, 2H, H^6), 4.21 (s broad, 2H, CH_2^4), 4.19–3.87 (m, 8H, OCH_2, CH_2^2), 3.59 (s broad, 2H, CH_2^1), 3.25 (s, 1H, C≡CH), 1.79–1.67 (m, 6H, OCH_2CH_2), 1.45–1.13 (m, 54H, $OCH_2CH_2(CH_2)_9CH_3$), 0.88–0.84 (m, 9H, $O(CH_2)_{11}CH_3$) ppm. ^{13}C-NMR (75 MHz, $CDCl_3$): $\delta = 170.6$, 168.1, 165.0, 155.6, 153.2, 150.5, 141.7, 128.7, 106.3, 90.0, 83.9, 75.3, 73.7, 69.6, 50.2, 43.8, 38.1, 32.1, 30.5, 29.91, 29.87, 29.85, 29.82, 29.75, 29.6, 29.54, 29.52, 26.29,

26.25, 22.9, 14.7. MS (ESI[+]): Calculated for $C_{53}H_{90}N_5O_6$ [M+H][+]: 892.68; found: 892.66 [M+H].

C2*: To a suspension of **C2.1** (250.0 mg, 0.9 mmol) in CH_2Cl_2 (15 mL), TFA was added (3.0 mL, 0.04 mmol), the resulting solution was stirred at room temperature for 3.5 h. Then, TFA was removed by coevaporation with CH_2Cl_2. The resulting solid was re-dissolved in CH_2Cl_2 (25 mL), then Et_3N (276.0 µL, 2.0 mmol) was added and the solution was stirred for 15 minutes. In another flask to a solution of the acid **W2*** (465.0 mg, 0.6 mmol) in dry CH_2Cl_2 (25 mL) at 0 °C, HOBt (162.0 mg, 1.2 mmol) and EDC (230.0 mg, 1.2 mmol) were added. The mixture was stirred for 15 minutes, then, the solution of the deprotected amine was added. The mixture was stirred at room temperature overnight. Once the reaction was completed, the solution was diluted with CH_2Cl_2 and then washed with HCl (0.1 N), $NaHCO_3$ (sat) and NaCl (sat). The phases were separated, and the organic layer was dried with Na_2SO_4 and then the solvent was evaporated. The crude product was purified by column chromatography, eluted with $CHCl_3$: MeCN (30:1) obtained **C2*** as a white solid (404.0 mg, 48%). ^{1}H-NMR (300 MHz, $CDCl_3$) $\delta = 9.01$ (m, 1H, N^3H), 7.87 (s broad, 1H, NH-H), 7.27 (s, 1H, CH^6), 7.05 (s, 2H, H^6), 6.94 (d, $J = 9.3$ Hz, 1H, N^5H), 5.56 (broad, 1H, NH-H), 5.09 (dd, $J = 6.9$, 9.3 Hz, 1H, H^4), 4.17–3.92 (m, 2H, CH_2^2), 3.60–3.58 (m, 2H, N^1CH_2) 4.02 (m, 6H, OCH_2), 2.96 (s, 1H, C≡CH), 2.15 (m, 1H, H^7), 1.88–1.64 (m, 6H, OCH_2CH_2), 1.54–1.19 (m, 54H, $OCH_2CH_2(CH_2)_9CH_3$), 1.04 (d, $J = 8.2$ Hz, 3H, CH_3^8), 1.02 (d, $J = 8.2$ Hz, 3H, CH_3^9), 0.89 (m, 9H, $O(CH_2)_{11}CH_3$) ppm. ^{13}C-NMR (75 MHz, $CDCl_3$) $\delta = 172.8$, 167.5, 164.9, 155.5, 153. 3, 150.5, 141.8, 129.3, 106.5, 89.8, 83.4, 77.3, 75.4, 73.8, 69.8, 58.7, 49.8, 37.20, 32.26, 32.08, 32.07, 30.5, 29.89, 29.85, 29.80, 29.74, 29.61, 29.59, 29.53, 29.51, 26.28, 26.25, 22.8, 19.5, 18.65, 14.24 ppm. MS (ESI[+]): Calculated for $C_{56}H_{95}N_5O_6$ [M+H][+]: 934.40; found: 935.75 [M+H][+]. $[\alpha]D_{20} = -1.21$ (c = 1, $CHCl_3$).

Synthetic procedures and characterization data for the new G—C final monomers (GC0, GC2 and GC2*, Schemes 1 and S3)

BC0: Following *Standard Procedure C*, **B**[12] (1.0 g, 1.56 mmol), **C0** (403.0 mg, 0.51 mmol), $Pd(Ph_3)_2Cl_2$ (6.8 mg, 0.01 mmol) and CuI (0.9 mg, 0.005 mmol) were dissolved in a THF:Et_3N mixture (15 mL). the resulting mixture was stirred at 40 °C overnight. Once the reaction was completed, the solvent was removed under reduced pressure. The resulting product was purified by column chromatography, using as eluent a $CHCl_3$:MeOH 50:1 mixture. The product was obtained as a colorless oil (345 mg, 55%). ^{1}H-NMR (300 MHz, $CDCl_3$): $\delta = 7.41$ (s, 1H, H^{6C}), 7.28 (s, 1H, $1H^b$), 6.85 (s, 1H, H^a), 6.78 (s broad, 1H, NH-H), 6.49 (s, 2H, H^2), 6.16 (bs, 1H, NH-H), 4.89 (s, 2H, CH_2^2), 4.04–3.89 (m, 10H, $OCH_2(CH_2)_{10}CH_3$, CH_2^c), 1.95–1.69 (m, 10H, $OCH_2CH_2(CH_2)_9CH_3$, CH_2^d), 1.67–1.52 (m, 2H, H_j), 1.46–1.08 (m, 70H, $OCH_2CH_2(CH_2)_9CH_3$, $CH_2^{f,g,h}$, $H^{e,i}$), 1.01–0.76 (m, 27H, $O(CH_2)_{11}CH_3$, $CH_3^{k,l,j}$). HRMS (ESI[+]): Calculated for $C_{75}H_{127}IN_3O_6$: 1292.8764 [M+H][+]. Found: 1292.8772 [M+H][+].

BC2: Following *Standard Procedure C*, **C2** (100.0 mg, 0.11 mmol), **B**[12] (115.3 mg, 0.34 mmol), $Pd(Ph_3)_2Cl_2$ (1.57 mg, 0.002 mmol) and CuI (0.2 mg, 0.001 mmol) were dissolved in a THF:Et_3N mixture. The solution was stirred at 40 °C overnight. The solvent was then removed under reduced pressure, and the resulting product was purified by column chromatography, using as eluent a $CHCl_3$:MeOH 100:1 solvent mixture. The product was obtained as a colorless oil (74.1 mg, 47%). ^{1}H-NMR (300 MHz, $CDCl_3$): $\delta = 8.32$ (s broad, 1H, NH^5), 7.44 (s, 1H, H^{6C}), 7.09 (s, 1H, H^b), 7.10 (s, 1H, H^a), 7.06 (s, 2H, H^6), 7.01 (s broad, 1H, NH-H), 6.75 (s, 1H, NH^3), 6.25 (s broad, 1H, NH-H), 4.22 (qd, $J = 16.3$, 5.7 Hz, 2H, CH_2^4), 4.02–3.89 (m, 10H, $OCH_2(CH_2)_{10}CH_3$, CH_2^c, CH_2^2), 3.76–3.60 (m, 4H, CH_2^d), 1.80–1.67 (m, 6H, $OCH_2CH_2(CH_2)_9CH_3$), 1.65–1.51 (m, 8H, H^e, CH_2^f, CH_2^1), 1.51–0.99 (m, 66H, $OCH_2CH_2(CH_2)_9CH_3$, $CH_2^{g,h}$, H^i), 0.86 (m, 27H, $O(CH_2)_{11}CH_3$,

ChemPlusChem

Communications
doi.org/10.1002/cplu.202100255

**Chemistry
Europe**
European Chemical
Societies Publishing

$CH_3^{i,j,k}$). HRMS (MALDI+): Calculated for $C_{79}H_{132}N_5O_8I$: 1406.9193 [M +H]$^+$. Found: 1406.9187 [M+H]$^+$.

B1C2*: Following *Standard Procedure C* for a Sonogashira coupling, **C2*** (200.0 mg, 0.214 mmol), **B1**[13] (627.2 mg, 1.07 mmol), Pd-(Ph$_3$)$_2$Cl$_2$ (3.0 mg, 0.004 mmol) and CuI (0.4 mg, 0.0002 mmol) were dissolven in a THF:Et$_3$N mixture (10 mL). The resulting solution was stirred at r.t. overnight, and then heated at 50 °C for 1 h. Once the reaction was completed, the solvent was evaporated under reduced pressure. The residue was then purified by column chromatography, using as eluent a CHCl$_3$:MeOH (100:1) mixture. The product was obtained as a white solid (140.0 mg, 47%). ^{1}H-NMR (300 MHz, CDCl$_3$) δ = 9.01 (m, 1H, N^{3}H), 7.87 (s broad, 1H, NH-H), 7.27 (s, 1H, CH^6), 7.20 (s, 1H, H^b), 7.05 (s, 2H, H^6), 7.03 (s, 2H, H^a), 6.94 (d, J= 9.3 Hz, 1H, N^{5}H), 5.56 (broad, 1H, NH-H), 5.09 (dd, J=6.9, 9.3 Hz, 1H, H^4), 4.17–3.92 (m, 2H, CH$_2^2$), 3.60–3.58 (m, 2H, N^{1}CH$_2$) 4.02 (m, 10H, OCH$_2$), 2.15 (m, 1H, H^7), 1.88–1.64 (m, 10H, OCH$_2$CH$_2$), 1.54–1.19 (m, 74H, OCH$_2$CH$_2$(CH$_2$)$_9$CH$_3$, OCH$_2$CH$_2$(CH$_2$)$_5$CH$_3$), 1.04 (d, J=8.2 Hz, 3H, CH$_3^8$), 1.02 (d, J=8.2 Hz, 3H, CH$_3^9$), 0.89 (m, 15H, O(CH$_2$)$_{11}$CH$_3$, O(CH$_2$)$_7$CH$_3$) ppm.

GC0: Following *Standard Procedure C* for a Sonogashira coupling, **BC0** (100.0 mg, 0.082 mmol), **G**[9] (80.0 mg, 0.097 mmol), Pd(Ph$_3$)$_4$ (2.226 mg, 0.002 mmol) and CuI (0.2 mg, 0.001 mmol) were dissolved in a THF:Et$_3$N mixture (3 mL). The mixture was stirred at 40 °C for 12 h. Once the reaction was completed, the solvent was evaporated under reduced pressure. The crude product was purified by column chromatography, using as eluent a CHCl$_3$:MeOH 100:1 mixture. The product was obtained as a yellow solid (48.9 mg, 30%). ^{1}H-NMR (300 MHz, CDCl$_3$): δ=7.64 (s, 1H, NH-H), 7.41 (s, 1H, H^{6C}), 7.13 (s, 1H, H^b), 7.01 (s, 1H, H^a), 6.79 (s, 2H, H$^{2'}$), 6.53 (s, 2H, H^2), 5.38 (s, 3H, CH$_2^{1'}$), 4.94 (s, 2H, CH$_2^1$), 4.21–3.82 (m, 20H, OCH$_2$(CH$_2$)$_{10}$CH$_3$, CH$_2^{c,d}$), 1.94–1.01 (m, 136H, OCH$_2$(CH$_2$)$_{10}$CH$_3$, CH$_2^{f,g,h}$, H^e, H^j), 1.01–0.75 (m, 36H, O(CH$_2$)$_{11}$CH$_3$, CH$_3^{i,k,l}$). HRMS (MALDI+): Calculated for C$_{127}$H$_{211}$N$_9$O$_{11}$Na: 2062.6153 [M+Na]$^+$. Found: 2062.6219 [M+Na]$^+$.

GC2: Following *Standard Procedure C* for a Sonogashira coupling **BC2** (100.0 mg, 0.071 mmol), **G**[9] (70.0 mg, 0.085 mmol), Pd(Ph$_3$)$_4$ (1.15 mg, 0.001 mmol) and CuI (0.1 mg, 0.0007 mmol) were dissolved in a THF:Et$_3$N mixture (3 mL) and stirred at 40 °C overnight. Once the reaction was completed, the solvent was removed under reduced pressure. The residue was then purified by column chromatography, using as eluent a CHCl$_3$:MeOH 100:1 mixture. The product was obtained as a yellow solid (100.5 mg, 67%). ^{1}H-NMR (300 MHz, CDCl$_3$): δ=7.98 (s broad, 1H NH^5), 7.75 (s broad, 1H, NH^3), 7.51 (s, 1H, H^{6C}), 7.13 (s, 1H, H^b), 7.03 (s, 1H, H^a), 6.99 (s, 2H, H^6), 6.80 (s, 2H, H$^{2'}$), 5.39 (s, 2H, CH$_2^{1'}$), 4.34–3.94 (m, 20H, OCH$_2$(CH$_2$)$_{10}$CH$_3$, CH$_2^{c,d}$), 3.89–3.70 (m, 6H, CH$_2^{4,2,1}$), 1.74–1.50 (m, 12H, CH$_2^{f,g,h}$), 1.49–0.96 (m, 112 H, OCH$_2$CH$_2$(CH$_2$)$_9$CH$_3$, H^e, H^j), 0.87 (m, 36H, O(CH$_2$)$_{11}$CH$_3$, CH$_3^{i,k,l}$) ppm. HRMS (ESI$^+$): Calculated for C$_{129}$H$_{215}$N$_{10}$O$_{12}$: 2097.6548 [M+H]$^+$. Found: 2097.6566 [M+H]$^+$.

GC2*: Following *Standard Procedure C* for a Sonogashira coupling, **B1C2*** (101.7 mg, 0.071 mmol, **G**[9] (72 mg, 0.087 mmol), Pd(Ph$_3$)$_4$ (1.15 mg, 0.001 mmol) and CuI (0.13 mg, 0.0007 mmol) in THF. Then a few drops of ^{i}Pr$_2$NH were added, and the solution was stirred at r.t. overnight. Once the reaction was completed, the mixture was filtered over a celite plug and washed with CHCl$_3$:MeOH 10:1. The solvent was then evaporated under reduced pressure and the residue was purified by column chromatography, using as eluent CHCl$_3$:MeOH 50:1. The product was obtained as a yellow solid (16 mg, 10%). ^{1}H-NMR (300 MHz, CDCl$_3$, TFA 1%) δ=7.96 (s, 1H, H^{6C}), 7.54 (s, 1H, H^b), 7.12 (s, 1H, H^a), 7.04 (s, 2H, H^6), 7.00 (s broad, 1H, NH^3), 6.80 (s, 2H, H$^{2'}$), 5.40 (s, 2H, CH$_2^{1'}$), 4.23–3.93 (m, 17H, OCH$_2$(CH$_2$)$_{10}$CH$_3$, H^4, OCH$_2$(CH$_2$)$_6$CH$_3$), 3.90–3.71 (m, 4H, CH$_2^2$, CH$_2^1$), 1.85–1.72 (m, 16H, OCH$_2$CH$_2$(CH$_2$)$_9$CH$_3$, OCH$_2$CH$_2$(CH$_2$)$_5$CH$_3$), 1.51–1.00 (m, 129H, OCH$_2$CH$_2$(CH$_2$)$_9$CH$_3$, OCH$_2$CH$_2$(CH$_2$)$_5$CH$_3$, H^7), 1.11–0.73

(m, 30H, O(CH$_2$)$_{11}$CH$_3$, O(CH$_2$)$_7$CH$_3$, CH$_3^8$, CH$_3^9$) ppm. HRMS (ESI$^+$): Calculated for C$_{128}$H$_{212}$N$_{10}$O$_{12}$: 2083.6391 [M+H]$^+$. Found: 2083.6391 [M+H]$^+$.

Conflict of Interest

The authors declare no conflict of interest.

[1] a) T. A. M. Bharat, L. R. Castillo Menendez, W. J. H. Hagen, V. Lux, S. Igonet, M. Schorb, F. K. M. Schur, H.-G. Kräusslich, J. A. G. Briggs, *Proc. Nat. Acad. Sci.* **2014**, *111*, 8233–8238; b) R. Dutzler, E. B. Campbell, M. Cadene, B. T. Chait, R. MacKinnon, *Nature* **2002**, *415*, 287–294.

[2] a) T. Komatsu, X. Qu, H. Ihara, M. Fujihara, H. Azuma, H. Ikeda, *J. Am. Chem. Soc.* **2011**, *133*, 3246–3248; b) S. Yuge, M. Akiyama, T. Komatsu, *Chem. Commun.* **2014**, *50*, 9640–9643; c) T. M. Fyles, *Acc. Chem. Res.* **2013**, *46*, 2847–2855; d) J. Montenegro, M. R. Ghadiri, J. R. Granja, *Acc. Chem. Res.* **2013**, *46*, 2955–2965; e) W. Si, P. Xin, Z.-T. Li, J.-L. Hou, *Acc. Chem. Res.* **2015**, *48*, 1612–1619.

[3] J. Couet, M. Biesalski, *Soft Matter* **2006**, *2*, 1005–1014.

[4] a) T. Yamamoto, T. Fukushima, T. Aida, in *Self-Assembled Nanomaterials II: Nanotubes* (Ed.: T. Shimizu), Springer Berlin Heidelberg, Berlin, Heidelberg, **2008**, pp. 1–27; b) S. Sim, T. Niwa, H. Taguchi, T. Aida, *J. Am. Chem. Soc.* **2016**, *138*, 11152–11155; c) S. M. Darnall, C. Li, M. Dunbar, M. Alsina, S. Keten, B. A. Helms, T. Xu, *J. Am. Chem. Soc.* **2019**, *141*, 10953–10957.

[5] a) B. Shen, Y. He, Y. Kim, Y. Wang, M. Lee, *Angew. Chem. Int. Ed.* **2016**, *55*, 2382–2386; *Angew. Chem.* **2016**, *128*, 2428–2432; b) W.-T. Chuang, T.-Y. Lo, Y.-C. Huang, C.-J. Su, U. S. Jeng, H.-S. Sheu, R.-M. Ho, *Macromolecules* **2014**, *47*, 6047–6054; c) I. W. Hamley, *Angew. Chem. Int. Ed.* **2014**, *53*, 6866–6881; d) T. Shimizu, *Bull. Chem. Soc. Jpn.* **2018**, *91*, 623–668; e) P. A. Rupar, L. Chabanne, M. A. Winnik, I. Manners, *Science* **2012**, *337*, 559–562.

[6] a) V. Vázquez-González, M. J. Mayoral, R. Chamorro, M. M. R. M. Hendrix, I. K. Voets, D. González-Rodríguez, *J. Am. Chem. Soc.* **2019**, *141*, 16432–16438; b) F. Aparicio, P. B. Chamorro, R. Chamorro, S. Casado, D. González-Rodríguez, *Angew. Chem. Int. Ed.* **2020**, *59*, 17091–17096; *Angew. Chem.* **2020**, *132*, 17239–17244; c) P. B. Chamorro, F. Aparicio, R. Chamorro, N. Bilbao, S. Casado, D. González-Rodríguez, *Org. Chem. Front.* **2021**, *8*, 686–696.

[7] a) M. J. Mayoral, N. Bilbao, D. González-Rodríguez, *ChemistryOpen* **2016**, *5*, 10–32; b) F. Aparicio, M. J. Mayoral, C. Montoro-García, D. González-Rodríguez, *Chem. Commun.* **2019**, *55*, 7277–7299; c) D. Serrano-Molina, A. de Juan, D. González-Rodríguez, *Chem. Rec.* **2021**, *21*, 480–497.

[8] a) C. Montoro-García, J. Camacho-García, A. M. López-Pérez, N. Bilbao, S. Romero-Pérez, M. J. Mayoral, D. González-Rodríguez, *Angew. Chem. Int. Ed.* **2015**, *54*, 6780–6784; *Angew. Chem.* **2015**, *127*, 6884–6888; b) S. Romero-Pérez, J. Camacho-García, C. Montoro-García, A. M. López-Pérez, A. Sanz, M. J. Mayoral, D. González-Rodríguez, *Org. Lett.* **2015**, *17*, 2664–2667; c) C. Montoro-García, J. Camacho-García, A. M. López-Pérez, M. J. Mayoral, N. Bilbao, D. González-Rodríguez, *Angew. Chem. Int. Ed.* **2016**, *55*, 223–227; *Angew. Chem.* **2016**, *128*, 231–235; d) C. Montoro-García, M. J. Mayoral, R. Chamorro, D. González-Rodríguez, *Angew. Chem. Int. Ed.* **2017**, *56*, 15649–15653; *Angew. Chem.* **2017**, *129*, 15855–15859; e) M. J. Mayoral, D. Serrano-Molina, J. Camacho-García, E. Magdalena-Estirado, M. Blanco-Lomas, E. Fadaei, D. González-Rodríguez, *Chem. Sci.*

2018, *9*, 7809–7821; f) C. Montoro-García, N. Bilbao, I. M. Tsagri, F. Zaccaria, M. J. Mayoral, C. Fonseca Guerra, D. González-Rodríguez, *Chem. Eur. J.* **2018**, *24*, 11983–11991; g) R. Chamorro, L. de Juan-Fernández, B. Nieto-Ortega, M. J. Mayoral, S. Casado, L. Ruiz-González, E. M. Pérez, D. González-Rodríguez, *Chem. Sci.* **2018**, *9*, 4176–4184.

[9] N. Bilbao, V. Vázquez-González, M. T. Aranda, D. González-Rodríguez, *Eur. J. Org. Chem.* **2015**, *2015*, 7160–7175.

[10] L.-C. Lee, Y. Zhao, *J. Am. Chem. Soc.* **2014**, *136*, 5579–5582.

[11] X.-L. Zheng, R.-R. Tao, R.-R. Gu, W.-Z. Wang, D.-H. Qu, *Beilstein J. Org. Chem.* **2018**, *14*, 2074–2081.

[12] A. Ajayaghosh, R. Varghese, S. Mahesh, V. K. Praveen, *Angew. Chem. Int. Ed.* **2006**, *45*, 7729–7732; *Angew. Chem.* **2006**, *118*, 7893–7896.

[13] C. Weder, M. S. Wrighton, *Macromolecules* **1996**, *29*, 5157–5165.

[14] a) N. Bilbao, I. Destoop, S. De Feyter, D. González-Rodríguez, *Angew. Chem. Int. Ed.* **2016**, *55*, 659–663; *Angew. Chem.* **2016**, *128*, 669–673; b) M. Martín-Arroyo, J. Castells-Gil, N. Bilbao, N. Almora-Barrios, C. Martí-Gastaldo, D. González-Rodríguez, *Chem. Commun.* **2021**, *57*, 1659–1662.

[15] a) J. Camacho-Garcia, C. Montoro-Garcia, A. M. Lopez-Perez, N. Bilbao, S. Romero-Perez, D. Gonzalez-Rodriguez, *Org. Biomol. Chem.* **2015**, *13*, 4506–4513; b) M. J. Mayoral, J. Camacho-Garcia, E. Magdalena-Estirado,

M. Blanco-Lomas, E. Fadaei, C. Montoro-Garcia, D. Serrano-Molina, D. Gonzalez-Rodriguez, *Org. Biomol. Chem.* **2017**, *15*, 7558–7565.

[16] H. M. M. ten Eikelder, A. J. Markvoort, T. F. A. de Greef, P. A. J. Hilbers, *J. Phys. Chem. B* **2012**, *116*, 5291–5301.

[17] a) M. J. Mayoral, C. Rest, J. Schellheimer, V. Stepanenko, G. Fernández, *Chem. Eur. J.* **2012**, *18*, 15607–15611; b) M. M. J. Smulders, M. M. L. Nieuwenhuizen, T. F. A. de Greef, P. van der Schoot, A. P. H. J. Schenning, E. W. Meijer, *Chem. Eur. J.* **2010**, *16*, 362–367; c) T. F. A. De Greef, M. M. J. Smulders, M. Wolffs, A. P. H. J. Schenning, R. P. Sijbesma, E. W. Meijer, *Chem. Rev.* **2009**, *109*, 5687–5754.

[18] S. Ogi, V. Stepanenko, K. Sugiyasu, M. Takeuchi, F. Würthner, *J. Am. Chem. Soc.* **2015**, *137*, 3300–3307.

[19] P. Iqbal, M. Mayanditheuar, L. J. Childs, M. J. Hannon, N. Spencer, P. R. Ashton, J. A. Preece, *Materials* **2009**, *2*, 146–168.